# Noise reduction, error analysis and experimental fiability for 3D deformation measurement with digital color holography

Silvio Montrésor, Pascal Picart
Laboratoire d'Acoustique de l'Université du Maine
UMR CNRS 6613, Le Mans, France 72085
Email: silvio.montresor@univ-lemans.fr

Oleksandr Sakharuk and Leonid Muravsky
Karpenko Physico-Mechanical Institute of the NAS
Ukraine, 5 Naukova str, Lviv 79601, Ukraine
Email: sakharuk@ipm.lviv.ua

*Abstract*—**This article presents an analysis of phase errors generated by advanced noise removal algorithms applied to phase maps obtained from digital holographic interferometry. The phase error is separated into two contributions that are the error generated by the denoising method and the error due to the phase noise. A comparison of several noise removal algorithms is presented according to four criteria to assess independently the two types of errors from simulated data. Application to 3D displacement fields measurement of composite material is presented.**

*Keywords*—*digital holography; phase error; speckle noise; denoising;*

## I. Introduction

Digital holography is an effective and robust method for imaging and metrology [1]. The measured field of interest is related to a wrapped modulo $2\pi$ phase map (also called phase fringe pattern). A limitation of digital holographic phase imaging is related to speckle decorrelation which occurs between two consecutive temporally varying digital holograms. This decorrelation adds a high spatial frequency noise to the useful phase data. Then, robust noise filtering has to be implemented in order to yield measured phase fringe patterns suitable for quantitative measurement. At the final step, the processed phase map has to be unwrapped in order to get a quantitative measurement of the measurand of interest (displacement, field, strain field, vibration field, etc). In this paper, we aim at comparing the performances of different advanced algorithms for phase denoising, consecutive residual error and systematic induced error. We propose to investigate denoising algorithms and to apply the optimal configuration to 3D displacement field measurement with digital color holography. The paper is organized as follows: in section II we introduce specificities of the speckle noise, in section III we introduce the methodology of this study, in section V results are discussed, and finally section V proposes application to 3D measurements.

## II. Basics of Speckle Phase Noise

Commonly, when the object under interest is distorted under any solicitation, which may be mechanical, acoustic, thermal, etc... a phenomenon of speckle decorrelation appears [1]. Its spatial correlation width is related to the size of the speckle grain in the amplitude image. Thus, the phase map requires a filtering process stage in order to be correctly exploited for a confrontation with a physical model of the studied object. The speckle decorrelation has been studied by some authors [2]. Phase decorrelation is described statistically by second order properties. Decorrelation can be highlighted from differences of two phases measured at two different instants. Raw hologram phase is random and has speckle properties because it is directly related to the roughness surface of the object illuminated by the laser. Correlation properties on phase or on phase differences are related to the second order probability density function of phase [2]. With variable $\beta = |\mu|\cos(\epsilon)$, the probability density function on phase noise $\epsilon$ is given by:

$$p(\beta) = \frac{1 - |\mu|^2}{2\pi}(1 - \beta^2)^{-3/2}(\beta \arcsin \beta + \frac{\pi\beta}{2} + \sqrt{(1 - \beta^2)}).$$

(1)

In (1), $|\mu|$ is the modulus of the complex coherence factor between the two speckle fields. Equation (1) describes the probability of noise $\epsilon$ in the phase difference between two instants. In this article, we present a comparison between various noise estimators. Generally, to preserve $2\pi$ phase jumps in the wrapped phase map, the processing is applied on sine and cosine of the phase variations. In order to evaluate the performances of de-noising and restoration, a realistic numerical simulation was developed. The goal of the simulation is to produce phase map corrupted by speckle decorrelation noise with the adequate probability density function (1). Details of such a realistic simulation are provided in [3]. Next section discusses on the methodology of this study.

## III. Methodology

In order to analyze errors induced by noise removing algorithms, we propose four indicators calculated from the phase maps obtained at different stages of the assessment. The chart is reported in Fig. 1. In the following, all quantities noted $\sigma_x$ are obtained as an estimation of the standard deviation of
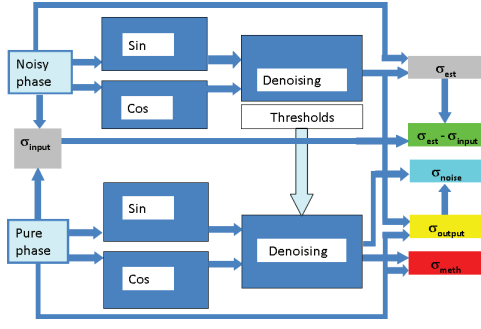
Fig. 1. Diagram charts of indicator computations.

a wrapped phase difference $\psi_{ab}$ ($\bar{\psi}_{ab}$ is the average phase difference) as:

$$\sigma_x = \frac{1}{NM} \sum_{i,j} (\psi_{ab}(i,j) - \bar{\psi}_{ab}(i,j))^2. \qquad (2)$$

In the above equation, $N$ and $M$ numbers define the size of the phase images; $\psi_{ab} = \phi_b - \phi_a$ is the wrapped optical phase difference calculated at two different states (or instants) of the object under interest. The first indicator is the global phase error after the denoising step $\sigma_{output}$. It is the standard deviation of the wrapped phase difference between the denoised phase and the exact reference noise-free phase. We call $\sigma_{intput}$ the global phase error before the denoising step. The second indicator is the phase error, noted $\sigma_{meth}$, due to the denoising method. It is computed from the wrapped phase difference between the denoised exact phase and the exact phase. It represents the amount of distortions only due to the denoising algorithm, without any noise contribution. Denoising algorithms as wavelet based methods need threshold values which are adjusted from a noise level estimator applied on the noisy phase. For these cases and as we can see on the computation chart Fig. 1, thresholds computed from noisy phase are kept to process the exact phase. The third indicator is the phase error, noted $\sigma_{noise}$ due to noise only. It is computed as the standard deviation of wrapped phase difference between the denoised phase and the denoised exact phase. At last, the fourth indicator is the estimation error of the input phase noise (not discussed further here). It is computed from the difference of the two quantities, $\sigma_{est} - \sigma_{input}$, where $\sigma_{est}$ is the estimated input phase error. The quantity $\sigma_{est}$ is computed from the wrapped phase difference between the denoised and the noisy phase.

## IV. DATABASE, EVALUATION AND DISCUSSION

We focuses on images of synthesized phases, in which one controls the fringe number and realistic phase noise [3]. For this evaluation, we selected algorithms known for their efficiency in the field of image processing: SAR algorithms (Synthetic Aperture Radar), algorithms based on wavelets [4], NLmeans and BM3D algorithms [5], windowed Fourier transform [6], anisotropic diffusion [7], curvelets [8], SPAD-EDH [9], Wiener filter method and finally median and Gaussian filters which are well known methods of classical spatial
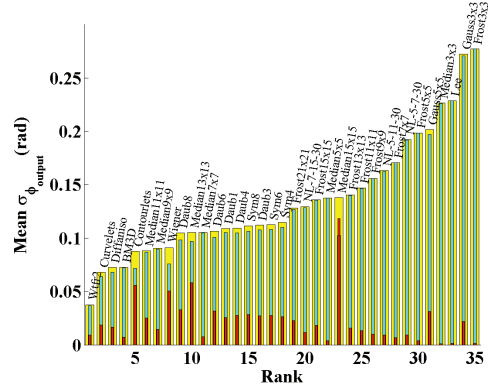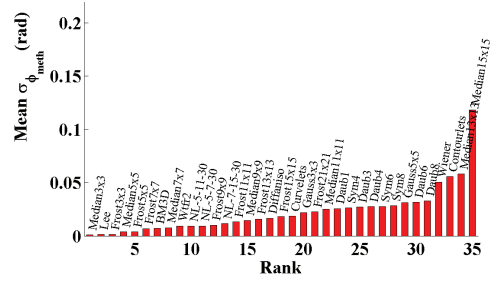


Fig. 2. Ranking of denoising algorithms.



Fig. 3. Ranking of errors induced by method only.

filtering. The evaluation results according to the output phase errors are reported in Fig. 2. The colors code is the same as that used in the computation chart (Fig. 1). The output error is represented by yellow bars. Inside the yellow bars, the blue bar represents the amount of noise error and the red bar represents the amount of method error. The displayed ranking is related to the output phase error. The ranking of denoising methods concerning the output phase error has been discussed in a previous paper [3]. So here the discussion is focused on the method and noise errors. First of all we can clearly see that the output phase error is less than the sum of the error method and the noise error. It is due to strong correlations existing between speckle noise and fringe interference structures. Concerning the median filters, we can see that the method error increases with the size of the neighborhood used to compute median values on phase maps. For a size of 15x15, the error method is greater than the error due to the noise: this is the only method in this case. Similar remarks can be made about Frost filters but with a method error which is always smaller, if we compare the same size of neighborhood. Stationary wavelet denoising methods present very closed results regardless of error types. We report in Fig. 3 the ranking of denoising algorithms concerning the error method. It confirms previous remarks about the influence of neighborhood sizes concerning Frost and median filters. The windowed Fourier transform (Wtfr2 in the bar graphs) is the best method for output error. For this method the ratio between method error and output is 26.24%. From our point of view this method constitutes
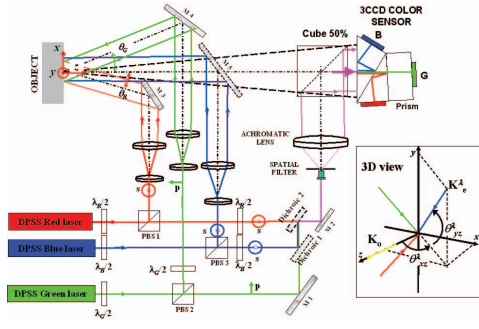
Fig. 4. Optical setup based on three-color digital holography

the best compromise for optimal denoising with minimizing filtering induced error.

## V. APPLICATION TO DIGITAL COLOR HOLOGRAPHY

Simultaneous 3D displacement field measurement can be achieved with digital three-color holography [10]. The experimental set-up is described in Fig. 4. It uses three lasers at three wavelengths (Red 632.8nm, Green 532nm, Blue 457nm). The object beams illuminate the sample under different incident angles, thus providing a simultaneous triple sensitivity to the 3D displacement field at the surface of the sample [10]. The sample (2mm×10mm×20mm) is put into a three-point bending test with progressive loading. The 3D displacement field $\{u_x, u_y, u_z\}$ at the sample surface can be extracted from the measurement of phase differences along the red, green and blue wavelengths [10]. The phase differences between two deformation states are calculated for each wavelength, then unwrapped and the three components of the displacement field are computed. The matrix relation between 3D displacement field $[U]$ and phase data $\Delta\varphi_\lambda$ provides relationship between the standard deviation of method error and that of each component of the displacement field. Fig. 5 illustrates experimental results. At each loading step, each R-G-B phase map is filtered by the Wtfr2 algorithm, unwrapped and the $\{u_x, u_y, u_z\}$ components are evaluated. Then the cumulated displacement field is obtained from each loading step. From filtering, the residual noise is estimated, and $26.24\%$ of this amount is considered to be due to the method error. From relationship between $[U]$ and $\Delta\varphi_\lambda$, the full contribution of the method error to the measurement can be estimated. With 8 loading steps to get the 3D displacement field in Fig. 5, the standard deviations are estimated to $\sigma_{U_x} = 0.373\mu m$, $\sigma_{U_y} = 0.439\mu m$, and $\sigma_{U_z} = 0.024\mu m$ respectively of each component. These values show that the method error is quite smaller than the amplitude of the displacement field ($\approx 6$ to $12\mu m$), thus providing high accuracy to the 3D measurement. The differences of errors along the three axes are due to spatial configuration beetween displacement vector and illumination geometry.

## VI. CONCLUSION

This paper presents a comparison between several image denoising algorithms in the context of speckle noise in phase
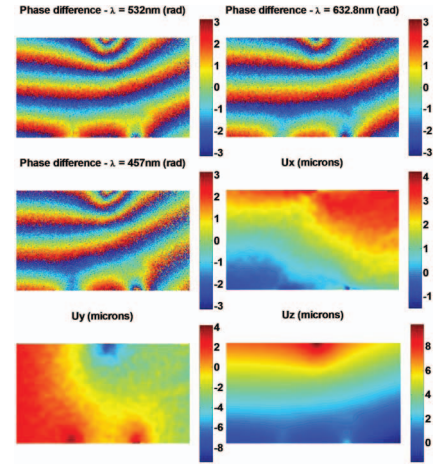


Fig. 5. Phase differences along R-G-B measurements and cumulated 3D displacement fields Ux, Uy, Uz.

data from digital holography. A ranking including 35 denoising algorithms is proposed. We have introduced the method error which represents the phase error induced by the denoising algorithm itself. The windowed Fourier transform denoising algorithm constitutes the best compromise between the output phase error and the method error. An application to 3D color digital holography to 3D deformation field composite characterization involving windowed Fourier transform is proposed. We show that the contribution of method error to the cumulated displacement filed is in sub-micrometer range, thus providing high accuracy to the measurement.

## REFERENCES

[1] P. Picart and J.C. Li, *Digital holography*, ISTE-Wiley, London, 2012.
[2] J. W. Goodman, *Speckle Phenomena in Optics*, Roberts and Company Publishers, Greenwood village, 2006.
[3] S. Montresor and P. Picart, "Quantitative appraisal for noise reduction in digital holographic phase imaging," *Opt. Express*, vol. 24, no. 13, pp. 14322–14343, June 2016.
[4] S. G. Mallat, *A wavelet tour of signal processing*, Academic Press, San Diego, 1999.
[5] V. Katkovnik K. Dabov, A. Foi and K. Egiazarian, "Image denoising with block-matching and 3d filtering," in *Proc. SPIE 6064*, 2006, vol. 14, pp. 1–12.
[6] Q. Kemao, "Windowed fourier transform for fringe pattern analysis," *Appl. Opt.*, vol. 43, pp. 2795–2702, 2004.
[7] P. Perona and J.Malik, "Space scale and edge detection using anisotropic diffusion," *IEEE Trans. on Pat. Anal. and. Mach. Int.*, vol. 12, no. 7, pp. 629–639, 1990.
[8] J.L. Starck, E. J. Candes, and D. L. Donoho, "The curvelet transform for image denoising," *IEEE Trans. Image Process.*, vol. 11, no. 6, pp. 670–684, June 2002.
[9] P. Memmolo, M. Iannone, M. Ventre, P.A. Netti, A. Finizio, M. Paturzo, and P. Ferraro, "Quantitative phase maps denoising of long holographic sequences by using spadedh algorithm," *Appl. Opt.*, vol. 52, no. 7, pp. 1453–1460, 2013.
[10] P. Tankam, Q. Song, M. Karray, J.C. Li, J.M. Desse, and P. Picart, "Realtime three-sensitivity measurements based on three-color digital fresnel holographic interferometry," *Opt. Lett.*, vol. 35, no. 12, pp. 2055–2057, 2010.